Laser Anemometer Measurements of Turbulence in Non-Newtonian Pipe Flows

J. S. CHUNG* AND W. P. GRAEBEL
Department of Engineering Mechanics, The University of Michigan, Ann Arbor, Michigan 48104
(Received 6 July 1970; final manuscript received 26 May 1971)

The structure of turbulence for pipe flows of dilute polyethylene oxide and polyacrylamide solutions is investigated using a laser anemometer technique. The instrumentation of the optical system and signal processing needed to satisfy the optical requirements and the signal-to-noise ratio are presented. The spatial requirement of the beam signal is described with regard to the lens, aperture, wavelength, and the angular alignment of the scattered and reference beams. A gravity-flow system is used to minimize the degradation of polymer solutions. The measurements of wall pressure drops indicate that the polymer additives used give a consistent delay of transition from laminar flow to turbulence, as compared with Newtonian fluids. The axial turbulence intensities for polymer solutions are found to be substantially reduced, compared with results obtained for water.

I. INTRODUCTION

In 1948, Toms[1] reported a large reduction in frictional drag in turbulent flows of fluids containing additives with high molecular weight (the so-called Toms effect). Since that time, even though considerable attention has been given to the flows of such fluids, the details of the mechanism which causes reduction in friction drag are not well understood for the non-Newtonian fluids involved. It has been suggested that the viscoelastic properties of these fluids may contribute to transition delay from laminar flow to turbulence, perhaps thereby decreasing the pressure losses in turbulent flow.[2] Also turbulence damping, thought to be due to viscoelastic properties of fluid,[2,3] has been observed, suggesting a further means of decreasing the pressure gradient. There are only a few measurements of the flow characteristics of non-Newtonian turbulent flow available in the literature. Seyer and Metzner[2] measured both axial and radial components of turbulence intensities by means of a series of photographs taken with small bubbles. Virk *et al.*[3] and Patterson and Zakin[4] measured only axial turbulence intensities with a hot-film sensor. These data showed a great deal of scatter and are not entirely satisfactory. Hot-film devices were found to be difficult to calibrate, and suffered from a buildup of material on the film.

In 1964 Yeh and Cummins[5] showed that fluid velocities could also be measured by means of a Doppler frequency shift caused in a monochromatic coherent light beam by scattering particles in a fluid. This Doppler-shifted frequency is linearly proportional to a component of the flow velocity at the point where light scattering occurs, allowing instantaneous measurements of velocity components at that point. The beams do not disturb the flow, and the measuring volume can be made very small by focusing of the beams. For these reasons, the optical heterodyne technique is a feasible and promising one, especially for the measurement of non-Newtonian flows in which additives cause extra problems for the use of conventional devices.

Instruments for such measurements in liquid flows have been introduced by Foreman *et al.*[6] and Goldstein *et al.*[7] The latter's geometry was used in the present work. The present optical system is briefly described in the next section with special regard as to how it satisfies the optical requirements. The instrumentation is described in greater detail elsewhere.[8]

A gravity-flow system is utilized instead of a pump-flow system. The gravity-flow system, as well as the technique used for preparation of polymer solutions, have the advantage of minimizing degradation effects in the polymer solutions. The present measurements are limited to axial turbulence intensities. The axial energy spectra obtained near the pipe centerline for polymer solutions differ only by relatively small amounts from those in Newtonian fluids. It is found that transition delay and axial turbulence damping take place consistently for all undegraded polymer solutions tested.

II. THE OPTICAL SYSTEM AND SIGNAL PROCESSING

A monochromatic beam of 1.5-mm diameter from a helium–neon laser (Jodon model HN-1576) is split by a beam splitter (BS in Fig. 1) into two beams. The beam passing through the beam splitter in the direction of the incident beam will be referred to as the scattering beam, and the beam reflected by the beam splitter will be referred to as the reference beam. The scattering and reference beams are made to meet at the point in the fluid where velocity is to be measured. Lenses (L1 and L2 in Fig. 1) are used to minimize the intersection point. The scattering beam is scattered by particles in the fluid. That portion scattered along the reference beam causes photomixing, or optical heterodyning, to take place on the photocathode of the photomultiplier tube. The Doppler frequency shift obtained by optical heterodyning is[7]

$$f_D = (2u/\lambda_r)\sin\theta, \tag{1}$$

where u is the velocity in the plane of the scattering and mixing beams and perpendicular to their bisector, λ_r is the laser wavelength (6328 Å in this case), and θ is the angle between the scattering and reference beams.

Several factors are important in designing and align-

ing an optical system for accurate measurement of f_D: (1) The spatial requirements of beams for photomixing,[9–12] which will be developed later, must be satisfied as closely as possible; (2) the optical system (optical table and devices, and photomultiplier tube and casing) should be stable and isolated from vibrations; (3) for measurement of axial velocity components the axis of the test section should lie in the optical plane, and the dividing line of the optical plane should be perpendicular to the axis of the test section; (4) the scattering volume desired should be exactly at a point of intersection of both beams, with both beams fully overlapping. To ensure satisfaction of Item (2), a granite optical table was mounted on massive supports and isolated from the flow system. Items (3) and (4) were accomplished by careful optical alignment.

To preserve the phase coherence in a Doppler-shifted beam, it is necessary to reduce the receiver aperture placed in front of the photomultiplier tube so that only a few diffraction lobes are incident on the photomultiplier cathode. By making the receiving angle such that the scattering volume size sustained at the distance P from the photomultiplier is equal to the diffraction limited angle β, Kroeger[10] obtained the following criterion,

$$1.22\lambda_r/l=\beta=d/P, \tag{2}$$

where β is the angular field of view of the photomultiplier, l is the photomultiplier aperture diameter, and d is the diameter of a scattering volume.

Angular misalignment between scattered and reference beams leads to a critical problem in photomixing. A method developed by Read and Fried[11] to reduce the spatial requirements by use of the Airy disk principle determines the disk diameter as

$$d=\lambda_r F/D, \tag{3}$$

where F is the focal length of a lens and D is the effective lens diameter.

The allowed angular tolerance in angular alignment of the scattered and reference beams is

$$\alpha=\pm D/\pi F. \tag{4}$$

The experimental results[11] on the output signal as a function of angular mismatch showed that they agreed well with the theoretical calculation. In order to maximize the signal-to-noise ratio an aperture approximately the size of the Airy disk should be used to block the portion of the reference beam that is not coincident with the scattered beam. This will eliminate the shot noise that would be produced by the unused portion of the reference beam. The use of focused beams requires careful positioning of the beams along the optical axis of the photomultiplier cathode. In the present experiment $D=0.155$ cm and $F=13.1$ cm (for the lens in front of the photomultiplier tube). The Airy disk

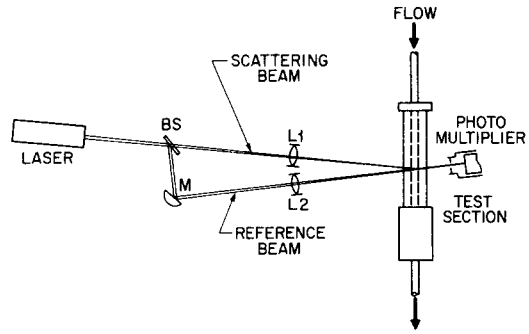

FIG. 1. Schematic of the optical system.

diameter and the angular tolerance were calculated from (3) and (4) to be $d=0.0535$ mm and $\alpha=\pm 0.00188$ rad. With the receiving aperture fully open to achieve the minimum photomixing, the maximum allowable angular misalignment according to (4) is $\alpha=0.00721$ rad, although the angular misalignment occurring in the experiment was at most 10^{-4} rad.

The scattering particles used were styrene/butadiene latex manufactured by Dow Chemical Co. These latex particles are spherical and of nonuniform sizes (average size 0.1985 μ). Their specific gravity is about 1.03 so it can be assumed that these latex particles follow the flow at very nearly the flow velocity. The chosen concentration of the scattering particles was $2.0\times10^{-2}\%$ of water by weight. Yeh and Cummins[5] showed that heterodyning of laser light scattered from regular polystyrene particles dispersed in water is feasible. Later, Foreman *et al.*[6] showed the feasibility of optical heterodyning with a laser beam scattered from particles of irregular size and shape. Homogenized dairy milk was tried in the present experiments and was observed to have a high light-scattering quality. However, long periods of dispersion in water caused the milk to spoil, presenting problems not found with the latex particles. The scattering volume was calculated from the Airy disk principle to be $d^3\sim10^{-6}$ cm^3.

Instantaneous flow velocity is defined as

$$u(t)=\bar{u}+u'(t), \tag{5}$$

where superposed bars denote time averages and primes denote fluctuations. Since Doppler-shifted frequency is linearly proportional to the velocity, Eq. (5) can be written in terms of the Doppler-shifted frequency as

$$f_D(t)=\bar{f}_D+f_D'(t). \tag{6}$$

Due to noise and variability in the scattered light intensity, the signal received by the photomultiplier is both amplitude and frequency modulated. It is thus difficult to obtain accurate values of $f_D'(t)$ from the signal processed through a wave analyzer which is both amplitude and frequency sensitive.[7,12] The received signal also contains frequencies from dc to the mega-

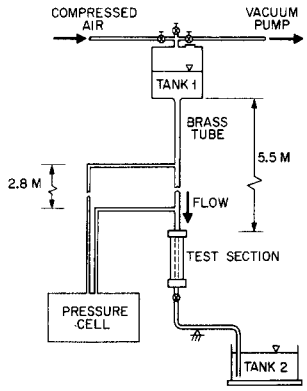

FIG. 2. Schematic of the flow system.

hertz range, imposing a further restriction on the use of wave analyzers for use in data conversion.

The photomultiplier output signals (always >3 mV rms) were instead fed into a read-out device manufactured by Laser Systems Electronics, Inc. (Laser Systems Signal Processor model 02A). Inside the read-out device, the photomultiplier signal is fed into a low pass filter (10-MHz cutoff) and then amplified in a wideband video amplifier. The phase of the heterodyned signal and the phase (1 MHz) of the voltage-controlled oscillator mix and produce a dc output voltage proportional to the phase difference (the oscillator frequency+Doppler frequency shift). Then this signal is amplified (dc–10 kHz) and filtered by a low-pass filter (10 kHz). This signal is read for data analysis with a dc voltmeter (Fairchild model 7050), and frequency counters (Hewlett-Packard models 5233L and 5512A). This read-out device is able to analyze the turbulence levels at frequencies of 10 kHz or lower. The read-out device by itself cannot suppress the low-frequency noise due to such things as building vibrations.

The energy spectra were obtained in the following way. The instantaneous velocity fluctuations were amplified to voltage levels of about 0.7 V rms and fed into a tape recorder (Ampex SP-300). These signals were later fed to a wave analyzer (Technical Products model TP627 T). Because of a short period of run (about 100 sec), the sweep rate in the spectrum analyzer was 27.5 Hz/sec for all flows tested.

III. FLOW SYSTEM CHARACTERISTICS

The general features of the equipment used to establish, control, and measure the flow are illustrated in Fig. 2. The top of the brass tube is a smooth continuation of a rounded, brass entrance section. The tube, which is 5.5 m long and has 1.19-cm i.d. (i.e., a length-to-diameter ratio of 461), is rigidly supported at the top, braced against lateral displacements 1.72 m from the top, and rigidly fastened to the top of the test section. An aluminum angle was clamped to the brass tube to further stiffen it. The test section was made of a Plexiglass block with rectangular outer surfaces and a cylindrical inner surface. Plexiglass was found to be a relatively effective optical material. The beam power loss was measured to be 13.6% for this test section filled with fresh tap water. To obtain velocity measurements at various distances from the center of the test section, the test section was moved by the adjustment of set screws along the horizontal line of the optical plane, coplanar with the scattered and reference beams. A fast-acting gate valve was located 15 cm below the test section and a length of copper tubing extended from the valve to the weighing tank. The device for positioning the scattering volume was calibrated by direct observation of the scattering volume with a microscope, and by using a geometrical correction for refraction.

For low rates of flow the static head was sufficient to drive the flow and the gate valve served as the flow regulator. In order to achieve higher rates of flow, tank 1 was pressurized, and the flow was controlled by adjusting the pressure in the tank in combination with the gate valve. The pressure in the tank was maintained at a preset value by a pressure regulator in the air supply line. The flow rate was determined by using a weighing scale and stop watch. The wall pressure drop along the tube was measured between two points 2.8 m apart by a differential-pressure transducer.

Flow rate Q (g/sec) was measured with a weigh scale and stop watch, and pressure drop Δp (dyn/cm^2) with a pressure cell (BLH model SR-4). Since the sample time for measurements varied between 2 and 4 min, the pressure head change during a run caused a small error in measuring both the flow rate and the pressure drop, which was corrected for. The solution temperature varied from test to test between 73 and 79°F, and all evaluation of quantities was based on the temperature of the individual solution, which remained very nearly constant during any given test.

The friction factor was calculated by

$$f=8\tau_w/\rho\bar{u}_N^2, \tag{7}$$

where $\tau_w=\frac{1}{4}D\,\partial p/\partial x$, ρ is the mass density of water, $\bar{u}_N=4Q/\rho\pi D^2 g$, D is the pipe diameter, and g is the gravity acceleration. The wall stress τ_w is frequently denoted in the literature by $\bar{u}_\tau=(|\tau_w|/\rho)^{1/2}$.

IV. POLYMER PREPARATION

Mechanical degradation usually occurs when polymer solutions are passed through a pump. To minimize this problem a vacuum system was employed to draw the fluid from tank 2 through the test section and brass tube into the reservoir, or tank 1, to permit reuse of the fluid. Two types of polymer powders were used; a polyoxyethylene (Union Carbide Polyox WSR-301 manufactured on 31 March, 1969, and used in August 1969) and a polyacrylamide (Separan AP30, Dow

Chemical, manufactured and used in 1969) with molecular weights 4×10^6 and 3×10^6, respectively. They are water soluble and tap water was used to prepare the polymer solutions. The highest concentrations used were 400 ppm (parts per million by weight) for Polyox WSR-301 solutions and 500 ppm for Separan AP 30 solutions.

The time required to prepare the uniformly dissolved polymer solutions in water depends on the mixing procedure. After several mixing trials, the procedure adopted was first to prepare a concentrated solution, and then to prepare the final solution by diluting the master solution to the desired concentration. To prepare a master solution, 8.67 liters of tap water were placed in a container and rocked slightly. A small amount of polymer powder was then sprayed onto the surface. The rocking was continued until the powder appeared thoroughly dissolved; a second application of powder was then sprayed on the surface and the process continued. After the concentrated solution had been prepared, test solutions of the desired concentration were readily prepared by diluting the master solution 10 to 1 with water. After approximately two hours the final solution appeared to the eye to be uniformly mixed, and had reached room temperature.

Polyox WSR-301 solutions were found to degrade faster and to a greater degree than Separan AP 30 solutions of the same concentration, due to both aging and shear. The Separan AP30 solutions showed no appreciable degradation during repeated test runs. Higher-concentration solutions of Polyox WSR-301 degraded more slowly than did low-concentration solutions. Although there were degradation problems with these solutions during turbulence measurement, the present gravity-flow system seems to cause less degradation than pumped-flow systems used by other investigators.

V. LAMINAR FLOW AND TRANSITION TO TURBULENCE

Delay of transition from laminar flow to turbulence for polymer solutions has previously been observed by

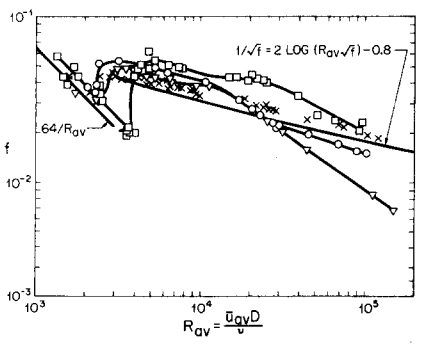

FIG. 3. Friction factor versus Reynolds number for water and aged dilute Polyox WSR-301 solutions: ×, water; ○, 10-ppm Polyox; □, 20-ppm Polyox; ▽, 100-ppm Polyox.

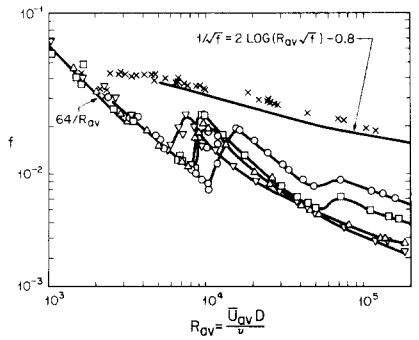

FIG. 4. Friction factor versus Reynolds number for water and fresh dilute Polyox WSR-301 solutions: ×, water; ○, 10-ppm Polyox; □, 20-ppm Polyox; △, 50-ppm Polyox; ▽, 100-ppm Polyox.

White and McEligot[13] and Hershey and Zakin.[14] The latter claimed an effect of pipe diameter on transition, i.e., the flow through a small diameter pipe increases the value of R_c, the Reynolds number at transition, to a higher value than that for flow through a large diameter pipe. They found that for polymer solutions the R_c for test pipes of both sizes are higher than that for water. They noted no appreciable degradation of the polymer solutions, and stated that transition delay took place even for very dilute solutions. It is noted, however, that ratios of the flow length to the pipe diameter, L/D, were not kept constant for the variations of D used in their experiments. Since the L/D ratio is important in determining the degree of flow development, unless sufficiently large L/D ratios are used, it is not completely certain that different values of R_c resulting from different L/D ratios were always due to the diameter effects of the pipe when the values of D were varied for the same value of L. There has also been a recent report[15] indicating that the friction factor varies significantly along the length of the pipe due to polymer degradation, affording degradations as another explanation for the diameter effect.

The tests for determining f as a function of R were made very carefully, especially near the transition region (Figs. 3, 4, and 5). Polymer solutions of Polyox WSR-301 and Separan AP30 of many different concentrations were used to determine if the characteristics of transition delay for the above polymer solutions are self-consistent. The present tests emphasize the effects of polymer degradation on transition delay for polymer solutions of different concentrations and of different periods of mixing.

For tap water, the critical Reynolds number for transition from laminar to turbulent flow for the apparatus used and the methods employed was found to be $R_c = 2395$. For fresh Polyox solutions, the range of R_c varied between 6428 and 10 570 depending on solution concentrations and age, as shown in Table I. For Separan solutions, the range of R_c was between 7850 and 13 920. For the Separan solutions used, and for the

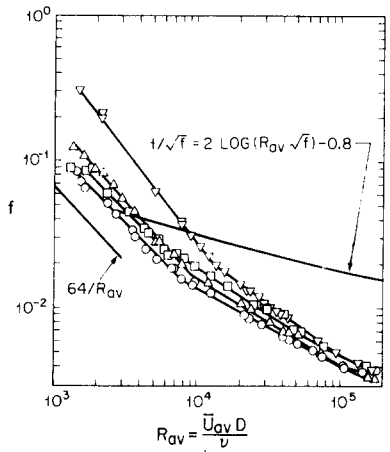

FIG. 5. Friction factor versus Reynolds number: ○, 100-ppm Separan AP30; □, 200-ppm Separan AP30; △, 500-ppm Separan AP30; ▽, 400-ppm Polyox WSR-301.

Polyox solution of 400 ppm, the velocity gradient, and hence shear stress, near the wall for laminar flow was larger than that for water, as shown in Fig. 6. For other solutions, the velocity gradient near the wall was essentially the same as that in water (Figs. 4 and 5).

As shown in Table I, or Figs. 4 and 5, transition from laminar flow to turbulence for Polyox solutions which were allowed to rest for periods shorter than one day before use took place at Reynolds numbers far beyond the critical Reynolds number obtained for unadulterated tap water. Solutions allowed to rest for longer than one day, when tested under the same conditions, were clearly affected by the aging of polymer solutions. For example, the values of R_c for fresh Polyox solutions of 10 and 100 ppm are about 10 000, but for aged solutions the values of R_c are almost the same as that for water. For all the test runs with polymers, viscosities as measured in a Cannon–Fenske viscometer were almost the same as tap water viscosity. The viscosity of tap water was used throughout in computing Reynolds number.

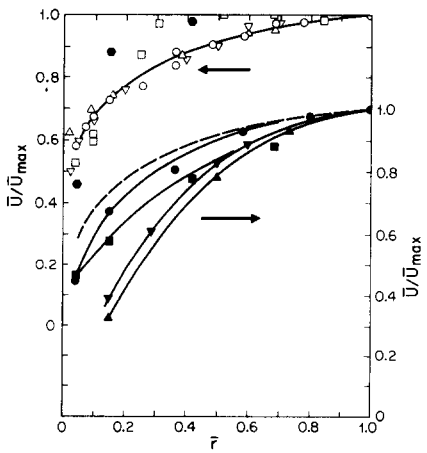

FIG. 6. Mean velocity distributions: ○ and – – –, water ($R_{max}=50\,400$); △, air (Laufer, $R_{max}=50\,000$); ▽, air (Sandborn, $R_{max}=50\,000$); □, 100-ppm Separan AP30 ($R_{max}=62\,200$); , 100-ppm Polyox WSR-301 ($R_{max}=52\,700$); ●, water ($R_{max}=25\,530$); ▲, 200-ppm Separan AP30 ($R_{max}=20\,400$); ▼, 200-ppm Separan AP30 ($R_{max}=17\,020$); ■, 100-ppm Polyox WSR-301 ($R_{max}=34\,800$).

TABLE I. Critical Reynolds number.

Type of polymer	Concentration (ppm)	Age of concentration solutions (h)	Age of diluted solutions (h)	Critical Reynolds numbers
Tap water	...	...	...	2 395
Polyox WSR-301	10	1.67	3.75	10 570
Polyox WSR-301	10	0.75	0.67	2 330
Polyox WSR-301	20	5.75	1	8 760
Polyox WSR-301	20	28	1.67	4 770
Polyox WSR-301	20	34	14	4 010
Polyox WSR-301	50	6.5	0.75	10 020
Polyox WSR-301	100	22	1.5	9 510
Polyox WSR-301	100	45	32	2 335
Polyox WSR-301	400	12	16	6 428
Separan AP30	100	1	3	7 850
Separan AP30	200	5	3	8 300
Separan AP30	500	6	3	13 920

There are sharp breaking points at the transition from laminar flow to turbulence of the Separan solutions seen in Fig. 5. The results obtained by White and McEligot,[13] however, show no sharp breaking points at transition for Separan solutions of very low concentration. It is known that some pseudoplastic solutions, such as carboxymethyl cellulose solutions and fiber suspension flows, show breaking points during their transition from laminar flow to turbulence. For Polyox solutions with concentrations between 10 to 100 ppm, the transition pattern from laminar flow to turbulence follows the pattern of water, having no sharp breaking point. For a Polyox solution of 400 ppm, however, the transition was found to have a sharp breaking point.

The effect of mechanical degradation on the polymer solutions is indicated in Table II, where drag reduction is shown as a function of the number of passes of the solution through the apparatus. The effect on Separan

TABLE II. Percent drag reduction as a function of passes through the system for $(Re)_m=5\times10^4$.

Polymer solution	Number of passes through system								
	1	2	3	4	5	6	8	10	12
Separan AP 30 (100 ppm)	78	74	74	74	74	74	73	...	...
Polyox WSR-301 (100 ppm)	78.5	72	65	55	52	...	...	...	...
Polyox WSR-301 (50 ppm)	72	71	67	62	...	52	50	44	40
Polyox WSR-301 (20 ppm)	60	51	62	41	...	...	...	...	...
Polyox WSR-301 (10 ppm)	60	44	27	21	...	...	...	...	...

TABLE III. Data for flow measurement $\{\bar{u}_\tau = [-\nu(d\bar{u}/dr)_{\bar{r}=0}]^{1/2}\}$.

Solution	R_{av}	$\bar{u}_{max}/\bar{u}_{av}$	$\bar{u}_\tau$ (cm/sec)	Age of concentrated solutions (h)	Age of diluted solutions (h)
Water	18 800	1.358	9.69	...	...
Water	38 300	1.316	18.7	...	...
Polyox WSR (20 ppm)[a]	41 800	1.35	17.9	28	17
Polyox WSR (20 ppm)[b]	53 900	1.038	16.2	21	2
Polyox WSR (50 ppm)	28 850	1.16	7.99	7	4
Polyox WSR (50 ppm)[b]	53 250	1.04	11.3	7	4
Polyox WSR (100 ppm)[b]	51 800	1.025	11.9	21	2
Polyox WSR (100 ppm)[b]	28 150	1.237	8.24	21	2
Separan (100 ppm)	51 300	1.21	10.8	2	1.5
Separan (200 ppm)	9 580	1.777	3.41	1.67	0.67
Separan (200 ppm)	13 830	1.477	4.48	1.67	0.67

[a] Degraded.
[b] Classified according to drag reduction percentage rather than their concentration in turbulence data.

was not as great as that on Polyox, which shows a marked amount of degradation upon repeated use.

It has been suggested[16] that the reason for this aging is that fresh polymer solutions are nonhomogeneous solutions of viscoelastic materials. There are large collections of the particles formed during preparation which have much greater elasticity than the ambient solutions. With time, or mechanical degradation, elasticity is lost due to the network of molecules being broken, until the properties of the ambient solution govern the flow. This mechanism then is much like the mechanism of turbulence suppression in the flow of fiber suspensions, in that increasing or decreasing the amount of flocculation in such flows has a pronounced effect on flow properties.

VI. TURBULENT FLOW

Measurements of turbulence quantities were made only on flows where $R_{max} > 10\,000$, since, as noted by others,[17] near transition turbulence levels were found to be very high and irregular. In the present experiments only axial components of velocity were measured. The data obtained show some scatter, due to the fact that as position in the pipe was varied, the exact value of the average velocity could not be reproduced. Additional difficulties were experienced near the wall due to reflections of the laser beam.

Mean velocity, $\bar{u}$, is directly converted with Eq. (1) from the measured Doppler-shifted mean frequency and shown in Fig. 6. The radial position $\bar{r}$ is defined as $\bar{r} = 1 - r/r_0$ where $r = 0$ at the pipe centerline and r_0 is the pipe radius. Since the flow rates were not precisely the same for all values of $\bar{r}$, mean velocities in Fig. 6 are corrected based on the $\bar{u}$ measured at the pipe centerline. The lowest Reynolds number used in the experiments for tap water is $R_{max} = 25\,530$ where R_{max} is based on the mean velocity at the pipe centerline, $\bar{u}_{max}$, and the pipe diameter, D. The normalized mean velocity distribution, $\bar{u}/\bar{u}_{max}$ versus $\bar{r}$ distribution for a Separan solution of 200 ppm at $R_{max} = 20\,400$ is seen to lie below the Polyox solution of 100 ppm. At $R_{max} = 17\,020$, the $\bar{u}/\bar{u}_{max}$ distribution for the above Separan solution is lower than that at $R_{max} = 20\,400$. In fact, for a Separan solution of 200 ppm $R_1 = 9580$ is close to its transition point. The ratio of centerline mean velocity to average velocity, $\bar{u}_{max}/\bar{u}_1$ near the transition of polymer solutions is higher than that found for water at the same Reynolds number, as shown in Table III. It is noted that $\bar{u}/\bar{u}_{max}$ distributions for Separan solutions of 200 ppm with $R_1 = 9580$ appear to be close to those for laminar flows.

Mean velocity profiles were consistently found to be blunter at high Reynolds numbers for non-Newtonian turbulent flows than for Newtonian flows at the same Reynolds number. The profiles shown in Fig. 6 for flows with polymer additives and $R_{max} \cong 50\,000$ show little variation of mean velocity with $\bar{r}$ for $\bar{r} > 0.3$. The value of $\bar{u}_{max}/\bar{u}_1$ was consistently found to be lower for the flows with additives than for water at the same Reynolds number, as shown in Table III. A similar result was obtained by Seyer and Metzner.[2]

Laser measurements of turbulence intensities near transition from laminar flow to turbulence were made by Goldstein[7] (only at the pipe centerline). He found that the turbulence intensities near transition were also higher than that in fully turbulent flow, and of the same level both for tap water and for a Polyox solution of 50 ppm which had lain for 24 h after having been mixed in a large batch. However, the present experiments show that the same Polyox solution which rested 24 h as a master solution before dilution barely shows drag reducing properties in turbulent flow (Fig. 3). The value of R_c for a Polyox solution which was prepared by the present method of mixing is seen from Fig. 4 to be markedly higher than that obtained by Goldstein. The axial turbulence intensities near the present transition are also higher than the ones he found in fully turbulent flows. The axial components of

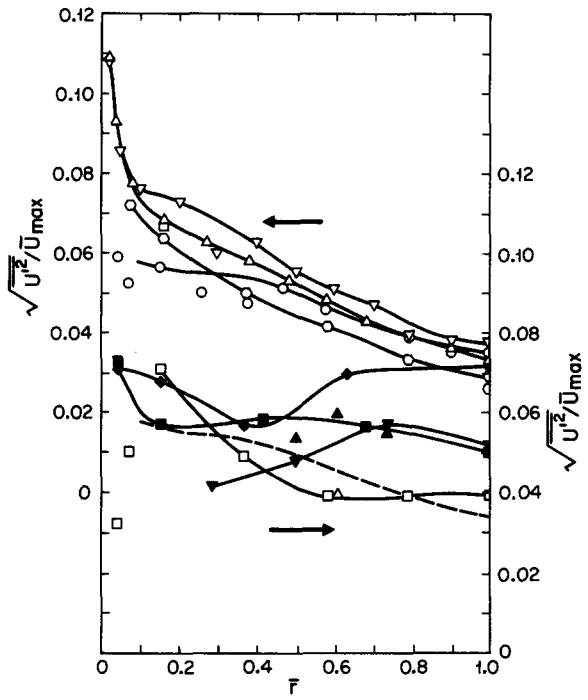

FIG. 7. Axial turbulence intensities: ○ and – – –, water ($R_{max}=50\,400$); △, air (Laufer, $R_{max}=50\,000$); ▽, air (Sandborn, $R_{max}=50\,000$); ▽, air (Laufer, $R_{max}=500\,000$); □, water ($R_{max}=25\,530$); ▼, 200-ppm Separan AP30 ($R_{max}=20\,400$); ▲, 200-ppm Separan AP30 ($R_{max}=17\,020$); , 50-ppm Polyox WSR-301 ($R_{max}=33\,600$); ■, 100-ppm Polyox WSR-301 ($R_{max}=34\,800$).

turbulence intensities found by Seyer and Metzner[2] are higher across the pipe radius near transition for both water and the polymer they used (ET-597) than for turbulent flow at higher values of the Reynolds number. Although their data shows a high degree of scatter, the trend of their turbulence intensities are in agreement with the present measurements.

Hot-wire measurements of axial turbulence velocity components by Laufer[18] and Sandborn[19] are compared with the present laser anomometer measurements at $R_{max}=50\,000$ in Figs. 6 and 7. The capacity of tank 1 allowed runs at $R_{max}=50\,000$ for a maximum period of 3 min. Only axial components of turbulence intensities, $(u'^2)^{1/2}/\bar{u}$, were measured. The errors in reading the rms values due to slight oscillations of the pointer of the rms meter at high frequencies were about 6% of the rms values. For $\bar{r}<0.072$ (close to the wall), high fluctuations in the rms reading were usual and in some cases caused a severe problem in reading rms values. As indicated previously, these errors were likely due to secondary light scattering between latex particles and the pipe wall. The errors due to pressure variations in tank 1 were about $\Delta R_{max}=\pm 3000$ for the flows at $R_{max}\geq 50\,000$.

Figure 8 shows that axial turbulence intensities for a Separan solution of 100 ppm are much lower than those for tap water for $\bar{r}>0.3$. Polyox solutions reveal the same phenomenon, as shown in Fig. 8. Wall shear stresses as well as flow rates were measured for all data points during turbulence measurements and are shown in Table III. Exact comparisons with others' turbulence data cannot be made because the polymers used by Virk *et al.*[3] and Patterson and Zakin[4] are different from the present one and the degree of their polymer degradation is not known. It is hard to compare the present turbulence data with Goldstein's,[7] unless his measurements of degradation for the Polyox solution of 50 ppm are known. Figure 8 indicates that axial turbulence intensities for a Polyox solution are indeed lower for $r>0.3$ than those for water, while near the wall they are generally higher. This is consistent for all polymer solutions which exhibit drag reduction. This result contradicts Virk's measurement[3] of high turbulence intensities, but agrees with low turbulence intensities measured by Seyer and Metzner.[2]

Seyer and Metzner measured turbulence intensities using the bubble technique and showed that the axial components of turbulence intensities were lower in polymer solutions than in water. Since ET-597 solutions showing a 55% reduction in drag show little degradation according to their results, and taking into account that their data showed a great deal of scatter, the level of axial turbulence intensities which they report seems to be roughly consistent with those found in the present experiments. Their measurements of radial turbulence intensities, $(\overline{v'^2})^{1/2}/\bar{u}_{max}$, did not differ from those for Newtonian fluids. If the level of $(\overline{v'^2})^{1/2}/\bar{u}_{max}$ measured by them indicates the correct trend, and if the phase relationship between u' and v' is as in the Newtonian case, the Reynolds shear stress would be smaller due to lower axial turbulence intensities.

It should be noted that the level of $(\overline{u'^2})^{1/2}/\bar{u}_{max}$ for a degraded Polyox WSR-301 solution of 20 ppm is about

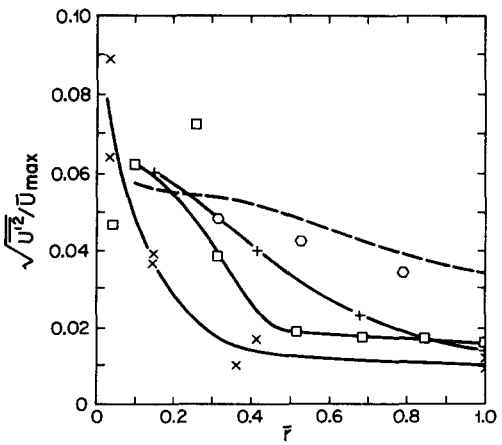

FIG. 8. Axial turbulence intensities: – – –, water ($R_{max}=50\,400$); □, 100-ppm Separan AP30 ($R_{max}=62\,200$); 20-ppm Polyox WSR-301 ($R_{max}=56\,400$); +, Polyox WSR-301, 50% drag reduction ($R_{max}=55\,000$); ×, Polyox WSR-301, 80% drag reduction ($R_{max}=55\,000$).

TABLE IV. Data for energy spectra $\{\bar{u}_\tau=[-\nu(d\bar{u}/dr)_{\bar{r}=0}]^{1/2}\}$.

Solution	$\bar{r}$	R_{av}	$\bar{u}_\tau$ (cm/sec)	Drag reduction (%)	Age of concentrated solutions (h)	Age of diluted solutions (h)
Water	1.0	41 700	18.9	...	...	...
	0.365	41 750	18.9	...	...	...
	0.015	42 000	19.1	...	...	...
Polyox WSR-301 (20 ppm)	1.0	58 850	17.2	45.6	14	12
	0.365	56 300	17.6	40.25	14	12
	0.015	56 800	17.4	40.8	14	12
Polyox WSR-301 (50 ppm)	1.0	51 500	10.0	75.8	8	2
	0.365	55 650	12.8	67.8	8	2
	0.042	55 800	15.2	62.0	8	2

the same as that for water (Fig. 8). Thus, damping of axial turbulence intensities for undegraded polymer solutions and the lack of damping of intensities for degraded polymer solutions seem consistent with the idea that axial turbulence damping is caused by an elastic property of polymer solutions. As indicated previously, this property also seems to cause transition delay.

Probably due to shear degradation the level of turbulence intensities for Polyox solutions was found to be not just a function of concentration in the present experiment. Rather, the percentage of drag reduction provides a better overall parameter to describe these solutions, and this is used in Fig. 8. Because they degrade less, Separan solutions are, however, classified according to their concentrations.

One-dimensional axial energy spectra are shown in wavenumber space for water in Fig. 9 and for Polyox solutions in Figs. 9 and 10 at different positions along the pipe radius. Details of flow properties are given in Table IV.

At $\bar{r}=0.015$, the measured $(\overline{u'^2})^{1/2}$ spectra for polymer solutions are higher in the low-wavenumber range than those found for water. At $\bar{r}=0.042$, the spectral distribution for a Polyox solution of 50 ppm is higher than

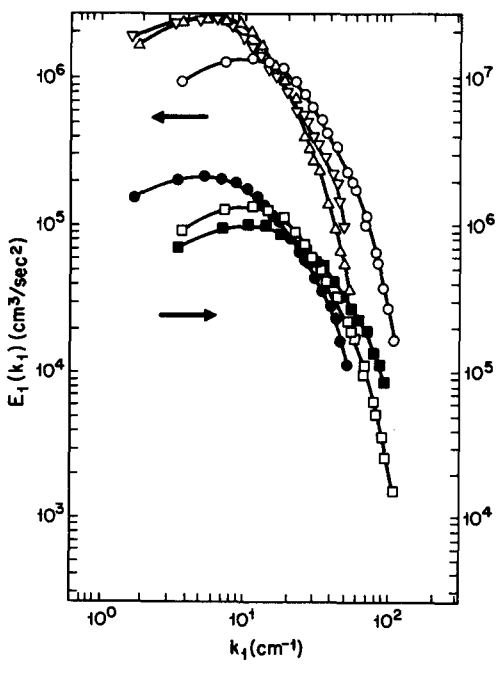

FIG. 9. Energy spectra for $(\overline{u'^2})^{1/2}$: ▽, water ($\bar{r}=1$, $R_{av}=41\,700$); △, water ($\bar{r}=0.365$, $R_{av}=41\,750$); ○, water ($\bar{r}=0.015$, $R_{av}=42\,000$); □, water ($\bar{r}=0.042$, $R_{av}=41\,700$); ●, 20-ppm Polyox WSR-301 ($\bar{r}=0.015$, $R_{av}=56\,800$); ■, 50-ppm Polyox WSR-301 ($\bar{r}=0.015$, $R_{av}=55\,800$).

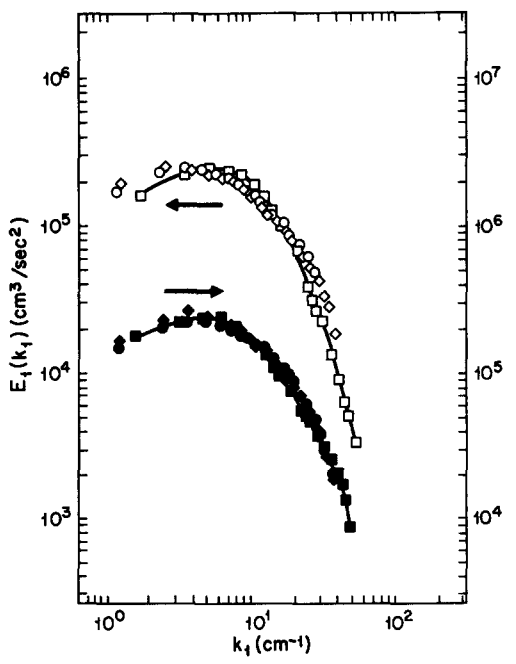

FIG. 10. Energy spectra for $(\overline{u'^2})^{1/2}$. □, water ($\bar{r}=0.365$, $R_{av}=41\,750$); ◇, 20-ppm Polyox WSR-301 ($\bar{r}=0.365$, $R_{av}=56\,300$); ○, 50-ppm Polyox WSR-301 ($\bar{r}=0.365$, $R_{av}=55\,650$); ■, water ($\bar{r}=1.0$, $R_{av}=41\,700$); ◆, 20-ppm Polox WSR-301 ($\bar{r}=1.0$, $R_{av}=58\,850$); ●, 50-ppm Polyox WSR-301 ($\bar{r}=1.0$, $R_{av}=51\,500$).

that obtained at $\bar{r}=0.015$ for water for k_1 between 32.8 and 75.4 cm^{-1} (Fig. 9). The spectra obtained at $\bar{r}=0.365$ for Polyox solutions are higher than those obtained for water while the spectra obtained at $\bar{r}=1.0$ are similar for water and polymer solutions.

VII. CONCLUSIONS

The turbulence data presented indicate that the laser anemometer technique is a promising one, especially for measurements of velocities in flows containing additives. The greater drag reduction and suppression of turbulence found for fresh solutions of Polyox WSR-301 are consistent with previous ideas as to the effects of nonhomogeneity of the solution, although the fact that aged or mechanically degraded solutions show these effects to a lesser degree indicates that this is not likely the only effect of the additive. Delay in transition to turbulence indicate that even well dissolved and homogeneous solutions show a marked effect on flow structure.

Since for Reynolds numbers greater than 40 000 flows with additives show blunter mean velocity profiles than water alone, it is quite possible that Reynolds stresses are also greatly reduced over that of water, at least in the interior of the pipe. Present efforts are to measure these stresses directly. The size of the apparatus used in the present experiments precluded obtaining measurements near the wall. The laser anemometer experienced difficulties in obtaining data near the wall due to reflections. To obtain such data, larger diameter tubes would help considerably.

ACKNOWLEDGMENTS

Scattering particles and the Separan AP30 used were kindly furnished by Dow Chemical Company.

This research was sponsored by the Office of Naval Research under Contract N000 14-67-A-0181-0030 with the University of Michigan.

* Present address: Esso Production Research Company, Houston, Texas 77001.

[1] B. A. Toms, in *Proceedings of the First International Rheological Congress*, (North-Holland, Amsterdam, 1949), Pt. 2, p. 135.
[2] F. A. Seyer and A. B. Metzner, Am. Inst. Chem. Engrs. J. **15,** 426 (1969).
[3] P. S. Virk, E. W. Merrill, H. S. Mickley, K. A. Smith, and E. L. Mollo-Christensen, J. Fluid Mech. **30,** 305 (1967).
[4] G. P. Patterson and J. L. Zakin, Am. Inst. Chem. Engrs. J. **13,** 513 (1967).
[5] Y. Yeh and H. Z. Cummins, Appl. Phys. Letters **4,** 176 (1964).
[6] J. W. Foreman, E. W. George, J. L. Felton, R. D. Lewis, J. R. Thornton, and H. J. Watson, IEEE J. Quantum Electron. **QE-2,** 260 (1966).
[7] R. J. Goldstein, R. J. Adrian, and D. K. Kreid, Ind. Eng. Chem. Fundamental, **8,** 498 (1969).
[8] J. S. Chung, PhD thesis, The University of Michigan (1969).
[9] M. Ross, *Laser Receivers* (Wiley, New York, 1966), p. 108.
[10] R. D. Kroeger, Proc. IEEE **53,** 211 (1965).
[11] W. S. Read and D. J. Fried, Proc. IEEE **51,** 1787 (1963).
[12] E. Rolfe, J. K. Silk, S. Booth, K. Meister, and R. M. Young, NASA CR-1199 (1968).
[13] W. D. White and D. M. McEligot, J. Basic Eng. (Trans. ASME) **92,** 411 (1970).
[14] H. C. Hershey and J. Zakin, Chem. Eng. Sci. **22,** 1847 (1967).
[15] R. W. Paterson and F. H. Abernathy, J. Fluid Mech. **43,** 689 (1970).
[16] V. N. Kalashnikow and A. M. Kudin, Izv. Akad. Nauk SSSR Mekh. Zh. Gaz. **1969,** 184.
[17] J. Rotta, Ing. Arch. **24,** 258 (1956).
[18] J. Laufer, NACA Report 1174 (1954).
[19] V. A. Sandborn, NACA TN 3266 (1955).